Scalable Lateral Mixing and Coherent Turbulence DRI: Use of an AUV to Quantify Submesoscale Mixing Processes

Louis Goodman
School for Marine Science and Technology (SMAST)
University of Massachusetts Dartmouth
706 South Rodney French Blvd
New Bedford, MA 02744
phone: (508) 910-6375 fax: (508) 910-6376 email: lgoodman@umassd.edu

Grant Number: N000140910173
http://www.smast.umassd.edu/Turbulence/

LONG-TERM GOALS

The long-term goal of this project is to understand the role of ocean turbulence in submesoscale dynamics.

OBJECTIVES

The objective of this project is to examine the role of ocean turbulence in submesoscale mixing observed during the June 2011 LatMix experiment. Key questions to be addressed are the following:

(1) What are the space and time statistics of breaking internal waves and how often do they result in turbulence?

(2) What is the role of fine scale intrusions in along and across isopycnal mixing? Is this the pathway of a forward cascade of energy and scalar variance from the submesoscale?

(3) What is the nature of the scalar spectra along isopycnals (dye, spice) between the submesoscale and the microscale ?

BACKGROUND

Central to quantifying ocean mixing is the relationship of essentially two dimensional QG like submesoscale variability, which produces along isopycnal mixing, to that of three dimensional turbulence, which produces across isopycnal mixing. Strongly related to this is the nature of the scalar variance spectral wavenumber cascade. Numerical studies such as that of Molemaker et al. (2005), and Thomas et al. (2007) suggest a forward scalar variance cascade within the submesoscale due to mesoscale straining. This is hypothesized to result in a "Batchelor" like -1 power law for the scalar variance wavenumber spectrum. Thus, a key factor in addressing the three original LatMIX hypotheses and in quantifying lateral along isopycnal mixing, is the nature of the scalar wavenumber spectra and the scalar variance cascade process. However, it should be noted that a very significant assumption is being made here, namely that there is stationarity and homogeneity over some (as of yet undetermined) space and times scale. An alternative viewpoint is that meso/submesoscale shear and straining can result in sporadic small scale intrusions which can lead to the pathway of small scale

Report Documentation Page

Form Approved
OMB No. 0704-0188

1. REPORT DATE	2. REPORT TYPE	3. DATES COVERED
30 SEP 2012		**00-00-2012 to 00-00-2012**

4. TITLE AND SUBTITLE	5a. CONTRACT NUMBER
Scalable Lateral Mixing and Coherent Turbulence DRI: Use of an AUV to Quantify Submesoscale Mixing Processes	5b. GRANT NUMBER
	5c. PROGRAM ELEMENT NUMBER
6. AUTHOR(S)	5d. PROJECT NUMBER
	5e. TASK NUMBER
	5f. WORK UNIT NUMBER
7. PERFORMING ORGANIZATION NAME(S) AND ADDRESS(ES) **University of Massachusetts Dartmouth,School for Marine Science and Technology (SMAST),706 South Rodney French Blvd,New Bedford,MA,02744**	8. PERFORMING ORGANIZATION REPORT NUMBER
9. SPONSORING/MONITORING AGENCY NAME(S) AND ADDRESS(ES)	10. SPONSOR/MONITOR'S ACRONYM(S)
	11. SPONSOR/MONITOR'S REPORT NUMBER(S)

12. DISTRIBUTION/AVAILABILITY STATEMENT
Approved for public release; distribution unlimited

13. SUPPLEMENTARY NOTES

14. ABSTRACT

15. SUBJECT TERMS

16. SECURITY CLASSIFICATION OF:			17. LIMITATION OF ABSTRACT	18. NUMBER OF PAGES	19a. NAME OF RESPONSIBLE PERSON
a. REPORT **unclassified**	b. ABSTRACT **unclassified**	c. THIS PAGE **unclassified**	**Same as Report (SAR)**	**12**	

diffusion and dissipation. Thus, a spectra approach at the submesoscale must be carefully formulated to take this into account. In addition, care must be taken to isolate the role that breaking internal waves play in this connection of submesoscale dynamics to that of turbulence.

A remarkable accomplishment of quasi equilibrium turbulence theory has been the development of the -5/3 law and – 3 law for the kinetic energy wavenumber spectra of 3D and 2D (QG) turbulence, respectively. These laws are based on ideas originally developed by A. N. Kolomogorov (1941) and then later by G. K. Batchelor (1953). Their experimental and numerical verification is one of the great scientific accomplishments of the past several decades. These spectral formulations are based on a combination of nonlinear cascade physics and dimensional analysis (Vallis, 2006). In the 3D turbulence case, the rate of transfer of kinetic energy (KE) is constant and equal to ε, the turbulent dissipation rate, with non linear 3 D processes resulting in KE being cascaded in the forward direction to smaller scales and higher wavenumbers. Note, however, that ε has two separate meanings. It is both the amount of kinetic energy which is eventually dissipated and it is also the rate of transfer of kinetic energy from larger turbulent scales to the mid range turbulent scales and then on to the smaller scales (Tennekes and Lumley, 1972). For the 2D QG turbulence case, as a result of potential vorticity conservation, non linear processes result in enstrophy being cascaded in the forward direction at some constant rate, ψ. This results in KE being cascaded in the inverse direction to larger scales and lower wavenumbers. Thus, ψ in QG turbulence plays the same type of role as a constant cascade parameter as ε does in 3D turbulence. It is straightforward to show that the rate of transfer of KE in QG, 2 D turbulence, ε, is not constant over this wavenumber regime.

These same quasi equilibrium cascade concepts can be applied to the scalar spectra. Let χ be the rate of transfer of some scalar such as temperature and salinity. If we assume an equilibrium subrange in which there is an imposed larger scale strain rate, S, on the scalar spectra, then χ must be constant in this wavenumber subrange. From just dimensional scaling the wavenumber scalar spectra Φ must take the form

(1) $$\Phi = A\frac{\chi}{S}k^{-1} \qquad \text{for} \qquad \kappa_u < \kappa < \kappa_l$$

(Kraichnan, 1967), where A is a universal constant of order 1; χ, the rate of transfer of scalar variance, has units $\frac{\textbf{(scalar units)}^2}{\textbf{time}}$ and S has units of (time)$^{-1}$. In this analysis we will take our spectra as referring to the 1D (measurable) horizontal wavenumber spectra.

In the 3D turbulent case the inertial subrange strain rate, S, must scale with the constant transfer rate of kinetic energy, ε, and only local wavenumber (Batchelor, 1953, Tennekes and Lumley, 1972), resulting in

(2) $$\Phi = A\frac{\chi}{\varepsilon}k^{-\frac{5}{3}} \qquad \kappa_e < \kappa < \kappa_v$$

while in the diffusive subrange S must scale with the local strain rate produced by the larger scale eddies in the inertial subrange resulting in

(3) $$\Phi = B\chi(\frac{\varepsilon}{\nu})^{-\frac{1}{2}}k^{-1} \qquad \kappa_\nu < \kappa < \kappa_B$$

where κ_e, is the energy containing wavenumber limit, κ_ν the Kolomogorv wavenumber limit, and κ_B ,the Batchelor wavenumber limit. Note that the constant B can be obtained in terms of A by setting the two forms of the wavenumber spectra given by (2) and (3) equal at the wavenumber boundary κ_ν. The well known and well verified spectral forms (2) and (3) represent the scalar inertial and diffusive subranges produced by 3D turbulence (Dillon and Caldwell, 1980).

These ideas can be extended to the submesoscale regime for the case of variability modeled as 2D QG turbulence. Taking S as the mesoscale strain rate we see that equation (1) then describes the scalar spectrum in the submesoscale which can be thought of as a "Batchelor" spectra with the mesoscale strain rate S replacing the 3D turbulent strain rate $(\frac{\varepsilon}{\nu})^{\frac{1}{2}}$ of equation (3). Recent results of Ferrari (ONR LatMIX Boston workshop, 2008) and others (Rudnick, 2001) suggest that "spice" spectra in the submesoscale follow the -1 power law of equation (1) and support theoretical concepts of Molemaker et al. (2005) and Thomas et al.(2007) and that it is the mesoscale strain rate S which results in the scalar variance forward cascade into the submesoscale.

Internal wave induced vertical displacements of a scalar gradient such as that of temperature and salinity can also result in scalar variability. One of the great accomplishments of the past 30 years has been the near universal nature of the Garrett and Munk (1975) model in describing IW spectral forms, although it should be noted that very limited horizontal spectral measurements of internal wave have been made. The GM models predict that scalar variance spectra would go as

(4) $$\Phi = E_\phi k^{-2} \quad \text{for} \qquad \kappa_0 < \kappa < \kappa_c ,$$

where κ_0 , κ_c are the wavenumber limits of the internal wave filed, determined by the source and sink of internal wave energy. In equation (4) E_ϕ has units of $\frac{\textbf{(scalar units)}^2}{\textbf{length}^{-1}}$. One of the most important recent theoretical and observational results is in relating GM type internal waves to turbulent dissipation rate, ε (Henyey, 1986, Gregg, 1989, Polzin, 1995) and that

(5) $$\varepsilon \propto E_\phi^{\,2}$$

This is related to the fall off of the spectra beyond $\kappa > \kappa_c$ where

(6) $$\Phi = \frac{E_\phi}{k_c}k^{-3}$$

From vertical microstructure profilers strong observational support for (5) and (6) occurs for the vertical 1D wavenumber spectra of temperature. No conclusive set of observations have shown the validity of (6) for the horizontal wavenumber spectrum.

However, recently Klymak and Moum (2007a,b) did attempt to examine the nature of the horizontal wavenumber spectra over the internal wave and submesoscale ranges of 1 m to 1 km. They found some limited evidence of (6) but for the most part observed that the horizontal wavenumber spectrum seemed to follow equation (2). This is an unexpected result since in this wavenumber regime 3D turbulence is expected to be highly anisotropic, which some have argued in analogy to the atmospheric case (Lumley, 1964,Weinstock,1985, Holloway, 1986) should result in a "buoyant" subrange with the spectra following a -3 power law as in equation (6). Moreover the type of measurements performed by Klymak and Moum (2007a, b), towing an instrumented body at 1 m/sec at essentially constant depth, are susceptible to finestructure contamination. This would result in flattening a -3 power law into a power law closer to -5/3 (Goodman, 1978).

Performing scalar measurements such as temperature and salinity along an isopycnal (spice) and at the same measuring the displacement of the isopycnal and the turbulent fields would be a clear way of distinguishing these mechanism and sorting out the different contributions of submesoscale variability, internal waves, and 3D anisotropic turbulence in producing along and across isopycnal mixing, which is critical to examining the nature of submesoscale mixing.

APPROACH

The observational approach has been to use the Autonomous Underwater Vehicle, T-REMUS, shown in Fig. 1. T-REMUS is a custom designed REMUS 100 vehicle manufactured by Hydroid Inc., containing the Rockland Microstructure Measurement System (RMMS), an upward and downward looking 1.2 MHz ADCP, a FASTCAT Seabird CTD, and a WET Labs BB2F Combination Spectral Backscattering Meter/ Chlorophyll Fluormeter. For the 2011 LatMiX experiment the BB2F system was configured with a Fluorescein sensor to detect the fluorescein dye deployments. In addition, the vehicle contains a variety of "hotel" sensors which measure pitch, roll, yaw, and other internal dynamical parameters.

This suite of sensors on T-REMUS allows quantification of the key dynamical and kinematical turbulent and submesoscale physical processes. The turbulence measurements are made concomitantly with very high spatial resolution measurements of velocity shear, temperature, salinity, and depth. The parameters which can be estimated from the data collected by the T-REMUS include: the turbulent velocity dissipation rate, ε, the temperature variance dissipation(diffusion) rate, χ, the local buoyancy frequency, N, and vertical shear, $\frac{du}{dz}$, and thus using the latter two quantities the Richardson (Froude) number $Ri = \frac{N^2}{(\frac{du}{dz})^2} = Fr^{-2}$. In addition we obtain simultaneously the local submesoscale fields of velocity salinity, density, fluorescein, chlorophyll-a and optical (700nm) scattering (Goodman & Wang, 2009; Wang & Goodman, 2009) in which the turbulence is embedded.

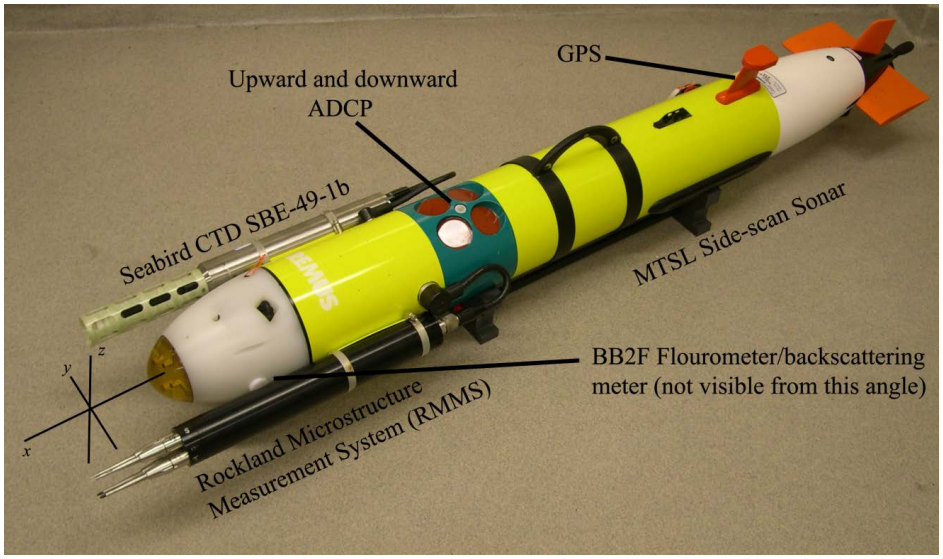

Figure 1, The SMAST T-REMUS Autonomous Underwater Vehicle. It is 2.0 m long, 20 cm diameter, and 63kg mass. Vehicle based sensors are indicated in the figure.

WORK COMPLETED

We carried out a very successful series of deployments of T-REMUS during the June LatMix 20011 experiment. In Figure 2 we show a schematic of the T-REMUS deployments. The T-REMUS was operated to make a series of box patterns around a drifting buoy drogued at 35 m depth. The idea was to follow the submesoscale flow field while simultaneously obtaining fine and microstructure (turbulent) data.

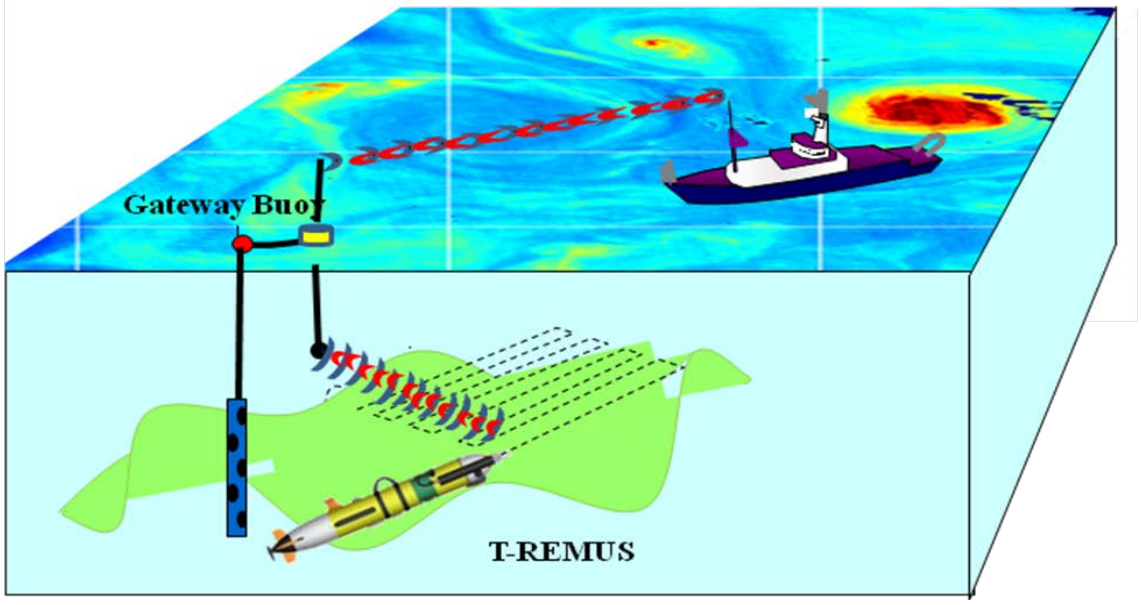

Figure 2, Schematic map of the T-REMUS deployments for the LATMIX DRI 2011 experiment. The T-REMUS AUV follows the Gateway Buoy by means of an attached drogued buoy .

To accomplish this type of deployment and track and communicate to and from the vehicle from our supporting ship, the Oceanus, we developed a unique three buoy system, shown in Figure 3. A leader buoy with a 10 m holey-sock drogue set between 30 to 40 meters was used to follow the flow field (be Lagrangian) at the approximate depth range of the dye deployments during LatMix 2011. The second buoy contained a thermistor chain set from 1 meter depth 49 meter depth containing 16 equally spaced therimsitors. An RBR CTD was set at the end of the T-chain and a depth sensor at the top of the chain. The third buoy contained the Hydroid communication "gateway" system. It was set to provide acoustic link from the buoy to the vehicle and then RF to the ship. We have subsequently added Iridium satellite communication capability.

Figures 3 Three buoy drogue Gateway Communication system used in LatMix 2011. The leader buoy has a 10 m holey-sock drogue centered at 10 m depth. The second buoy contains a 16 element thermistor chain spanning 1m to 49 m. The third buoy is the hydroid Gateway communication buoy.

In Figure 4 we show the times and locations of the deployments made between 3 June 2011 and 18 June 2011. Also shown are the actual tracks of the T-REMUS, both in absolute and relative coordinates.

Data Analysis and Preliminary Results

Much of the work following the 2011 field deployments was in reducing the enormous amount of data taken to a usable scientific format. As of this writing, over 50 % of this phase has been completed. Preliminary analysis has been initiated on the second half of the 2011 LatMix experiment when the T-REMUS via our three buoy system intruded into a frontal zone. We have also written a number of new analysis routines. We have developed, following Winters and D'Asaro (1996), a three dimensional sorting algorithm to obtain turbulent patch statistics. We will present below some of our results to date.

LatMix T-REMUS Deployments

Date in	06/03/11	06/05/11	06/08/11	06/10/11	06/14/11	06/16/11	06/18/11
Time in (UTC)	06:03:14 PM	02:34:42 PM	05:46:34 PM	11:32:09 AM	01:17:11 PM	01:03:08 PM	01:03:24 PM
Time out (UTC)	08:25:23 PM	10:50:43 PM	11:16:32 PM	09:44:37 PM	10:57:00 PM	10:58:05 PM	08:23:43 PM
Starting Longitude	-72.7449	-73.1243	-73.021	-72.9881	-73.0789	-73.5908	-74.1988
Starting Latitude	31.99	32.0734	31.9384	31.7897	32.5184	33.0707	33.887
Ending Longitude	-72.7407	-73.1082	-73.019	-73.0147	-73.1451	-73.7004	-74.2319
Ending Latitude	31.9744	32.0842	31.9196	31.7416	32.6475	33.2104	34.0078

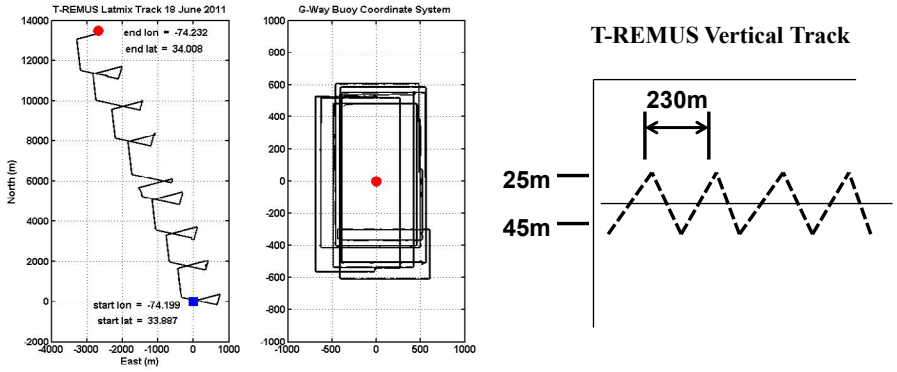

Figure 4 T-REMUS deployment times and tracks.

From 14 June to 18 June our 3 buoy system drifted into an increasingly stronger mesoscale field with both shear and strain variability increasing. Figure 5 shows a satellite derived map of SST and our Gateway buoy tracks.

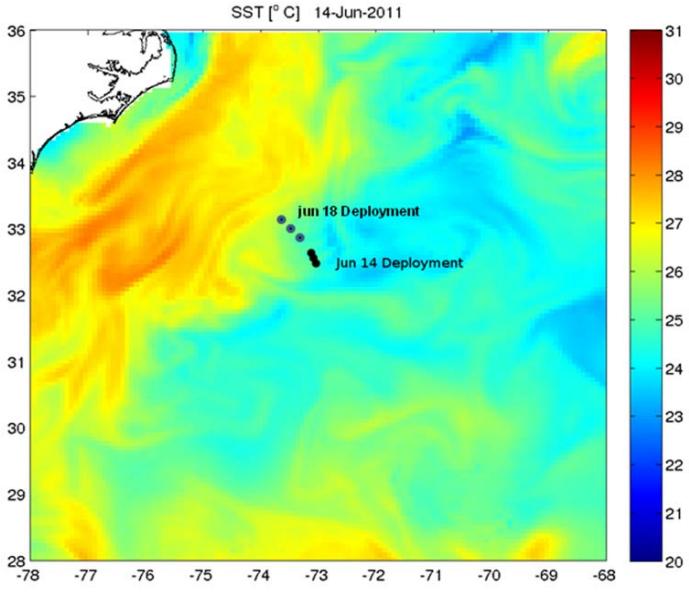

Figure 5 Track (dotted circles) of the 3 buoy system from 14 June 2011 to 18 June 2011 overlaid on SST map.

In figure 6 we show a contour map of salinity obtained from the T-REMUS CTD on 18 June 2011. The vertical axis is density and the horizontal axis is the along track location of the observations in a fixed earth coordintate system. Note that density for this environment is mainly determined by temperature so that salinity can be used approximately as a passive tracer, although there are some instances where double diffusion effects can occur. Figure 6 clearly shows three distinct regions, which are labelled in the Figure. Region 2 indicates a cold fresh intrusion. Toward the end of the run starting at approximately 10 km downstream frontal strucutre is observed.

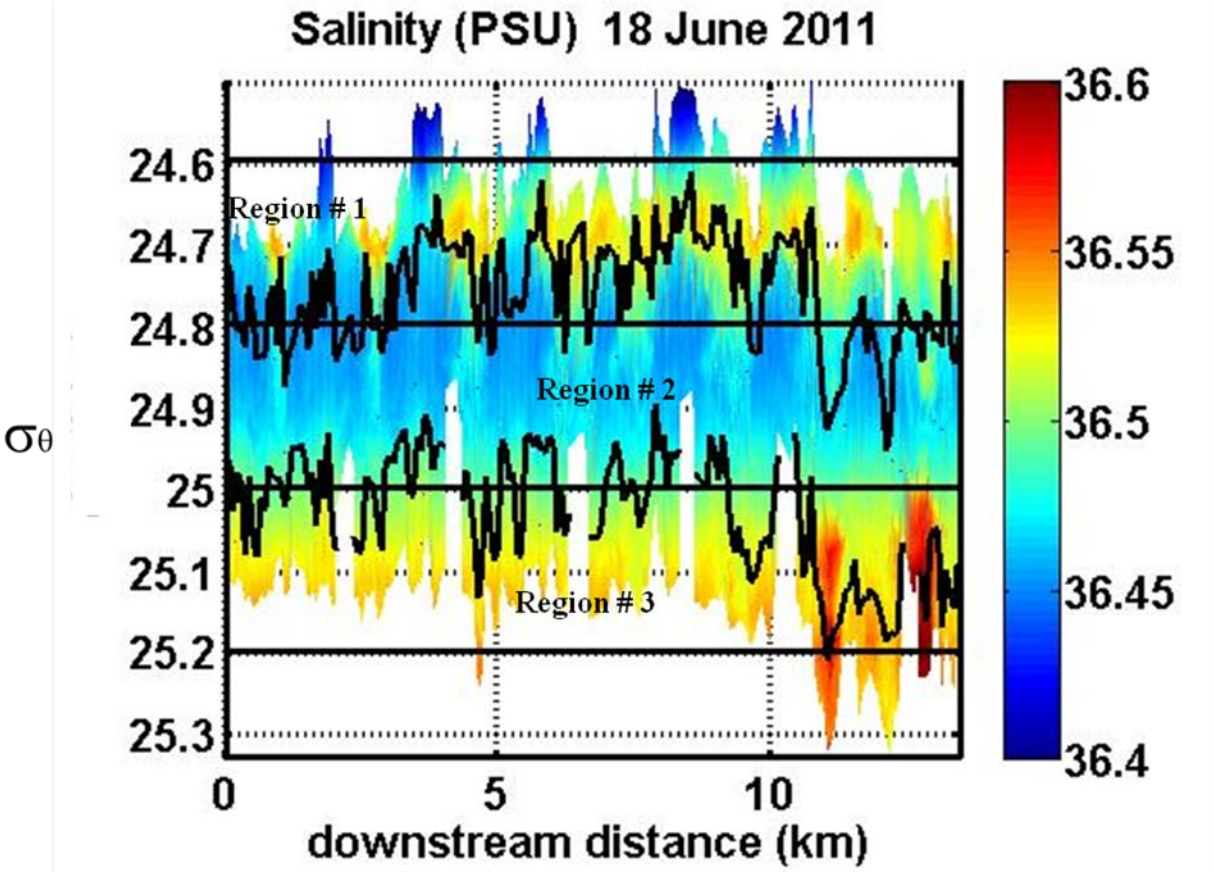

Figure 6 contour map of Salinity as a function of density and downstream distance obtained from the t-REMUS CTD.

In Figure 7 we show a contour map of χ the rate of molecular diffusion of temperature (heat). Note how the larges values are typically along the edges of the intrusions,i.e region # 2.

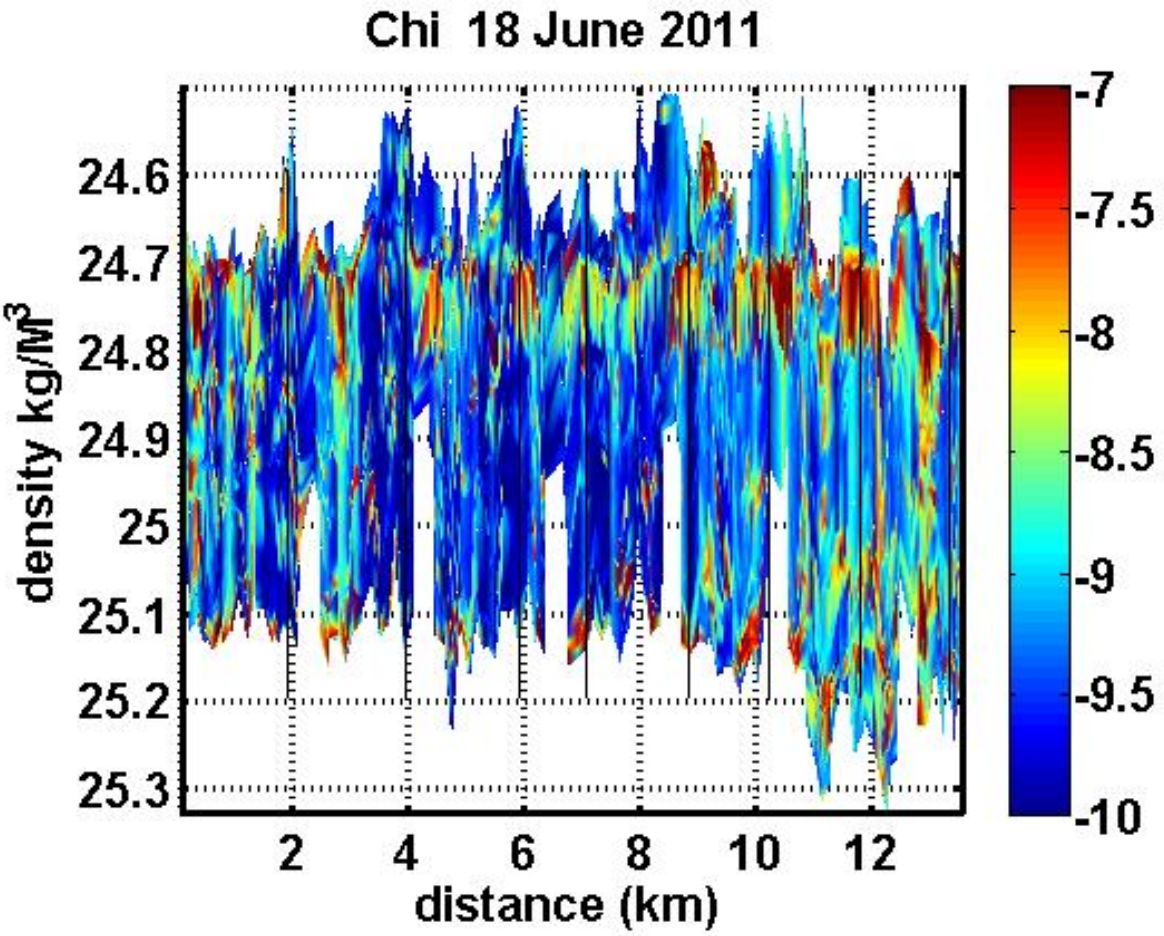

Figure 7 Contour map of χ as a function of density and downstream distance

Following the approach of D'Asaro (3008) we have examined the along isopycnal mixing using a density coordintate system. The unqiue combination of data obtained by the T-REMUS vehilce, ε,χ and finescale gradients, both along and across isopycnals of T ansd S allows us to calculate a temprature budget in density coordintates (McDougall, 1984) This is shown in Figure 8. We see that the along isopycnal diffusivity can reach vaues of order 10 m^2/sec, a value comparable at times with the with LatMix 2011 dye estimate during the same time of deployment. Thus our tentative conclusion to date is that samll scale intrusions (vertical sclaes of 10-15 m and horizontal scales of order kilometers) can play a very signficant role in along isopycnal mixing and should be taken into acount in numerical models.

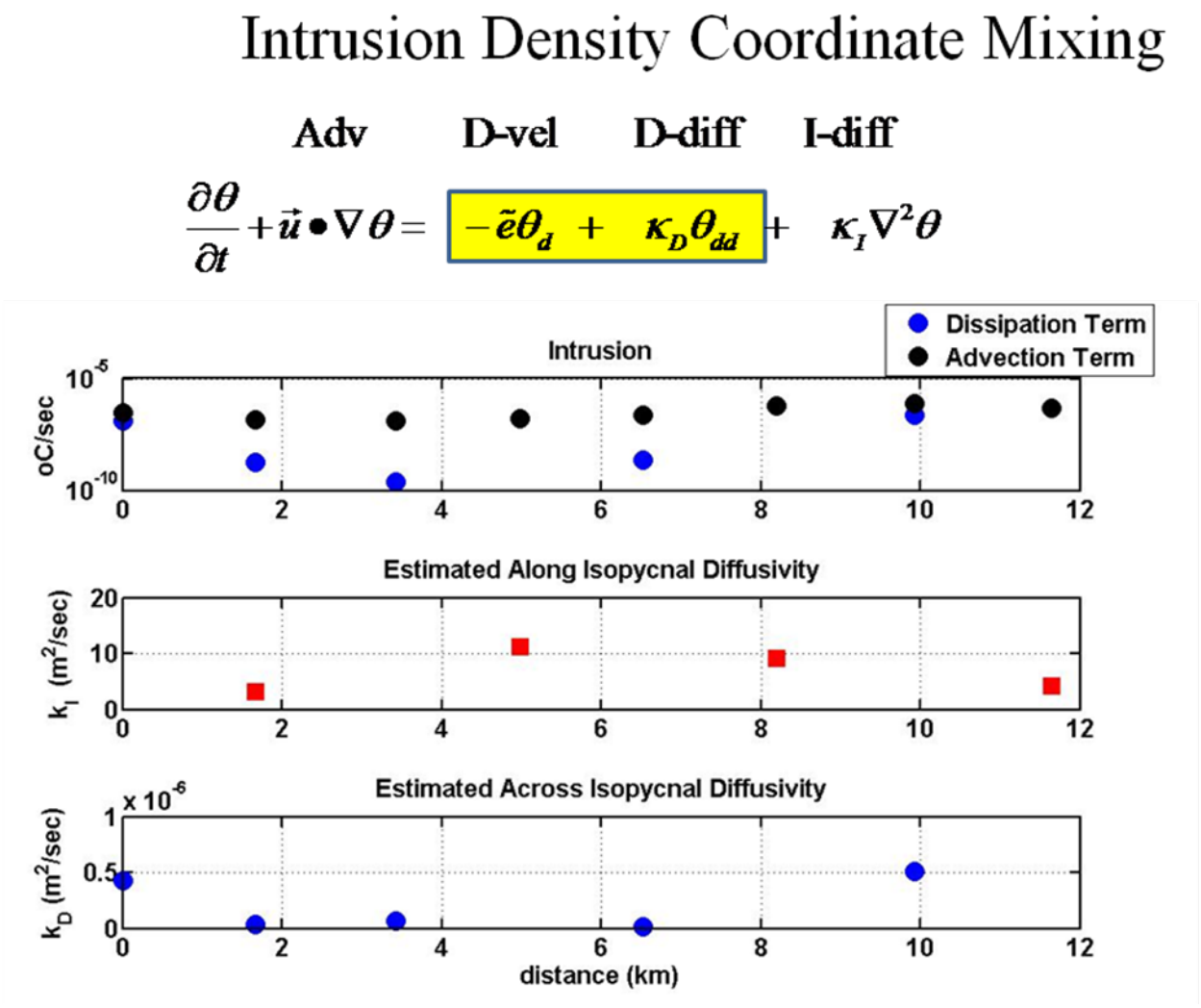

Figure 8. Top the advction diffusion equation in density coordinates. Bottom 3 paels indicat: (the dissipation term (shown in yellow in the above equation) and the along isopycnal diffusion term (I-diff).The lower two panels are the along and across ispoycnal diffusivities.

REFERENCES

Batchelor, G.K. Theory of homogenous Turbulence, Cambridge University Press, 1953

D'Asaro, E.A.,A diapycnal mixing budget on the Oregon shelf, Limnol. Oceanogr., 53(5, part 2), 2008, 2137–2150

Dillon, T. M., and D. R. Caldwell, 1980: The Batchelor spectrum and dissipation in the upper ocean. *J. Geophys. Res.,* **85,** 1910–1916.00

Garrett ,C.J.R. and W. H. Munk, 1975, Space-time scales of internal waves: A progress report, J. Geophys. Res. 80, 291-297

Goodman, L. 1978, On the Time Dependence of a Scalar Undergoing Advection, J. PHYS. Oceanogr., Vol. 8, No.5.

Goodman, L. , E. Levine, and R. Lueck, 2006, On Closing Turbulence Budgets from an AUV, J. Atoms. Ocean. Tech. 23, 977-990, July 2006

Goodman, L. and Robinson, A.R. On the Theory of Advective Effects on Biological Dynamics in the Sea, III: The Role of Turbulence in Biological Physical Interactions, Proc Royal Soc., Proceedings A 464 (2091), Mar 08, 2008.

Goodman, L. and Z. Wang, June, 2009, Turbulence observations in the northern bight of Monterey Bay from a small AUV, Journal of Marine Systems, Volume 77, Issue 4, Special issue on marine turbulence, p441-458, ISSN 0924-7963, Doi:10.1016/j.jmarsys.2008.11.004

Henyey, F.S.J., J. Wright, and S.M. Flatte, 1986, Energy and Action flow through the internal wave field, j. Geophys. Res., 91, 8487-8595

Holloway, G., 1986: Considerations on the Theory of Temperature spectra in Stably Stratified Turbulence. *J. Phys. Oceanogr.*, **16**, 2179–2183.

Klymak, J.M., and J.N. Moum, 2007a: Oceanic Isopycnal Slope Spectra. Part I: Internal Waves. *J. Phys. Oceanogr.*, **37**, 1215–1231.

Klymak, J.M., and J.N. Moum, 2007b: Oceanic Isopycnal Slope Spectra. Part II: Turbulence. *J. Phys. Oceanogr.*, **37**, 1232–1245.

Kolmogorv, A.N., 1941, The local structure of turbulence in an incompressible viscous fluid for very large Reynolds numbers, C.R. Akad Nauk,SSR, 30 301-305

Kraichnan, R.H. 1967 Inertial ranges in two dimensional turbulence, Phys. Fluids, 10 1417-1423

Lumley,J.L. 1964 The spectrum of nearly inertial turbulence in a stably stratified fluid. J. Atmos Sci. 21, 99-102

MacDonald, D. G., L. Goodman, and R. D. Hetland, 2007, Turbulent dissipation in a near-field river plume: A comparison of control volume and microstructure observations with a numerical model , *J. Geophys. Res.*, 112,

McDougall, T. J. 1984. The relative roles of diapycnal and isopycnal mixing on subsurface water mass conversion, J. Phys. Oceanogr. 14: 1577–1589.

Molemaker, M. J., J. C. McWilliams, and I Yavneh, 2005, Baroclinic instability and loss of balance, J. Phys. Oceanogr., 35, 1505-1517

Polzin,K.L.,J.M. Toole, R.W Shmitt, 1995, Finescale Parameterization of turblent dissipation, J. phys. Oceanogr. 25, 306-328

Rudnick, D.L., 2001, On the horizontal variability of the upper ocean, Proceedings Hawaiian Winter Workshop [12th] Held in the University of Hawaii at Manoa on January 16-19, 2001, 87-94.

Tennekes, H. and Lumley, J. L. A First Course in Turbulence, MIT Press, 1972

Thomas, L. N. Tandon, A., Mahaedevan, A., Submesoscale processes and dynamics, submitted 2007 J. Gepoophys. Res

Vallis, G.K. 2006, Atmospheric and Oceanic Fluid Dynamics: Fundamentals of Large-scale Circulation, Cambridge University Press

Wang, Z. and L. Goodman, January, 2009, Evolution of the spatial structure of a thin phytoplankton layer into a turbulent field. Marine Ecology Progress Series. 374:57-74 Doi:10.3354/meps07738.

Weinstock, J. 1985 On the Theory of temperature spectra in a stratified fluid, J. Phys. Oceanogr., 15, 475_477

Winters K.B. and D'Asaro, E. A., 1996, Diascalar flux and the rate of fluid mixing, J. Fluid Mech., vol 317, pp.179-193